THE ENERGY SPECTRUM OF FISSION NEUTRONS FROM 235

W. E. Bennett and H. T. Richards
The Rice Institute

October 30 1942

ABSTRACT

A cloud chamber has been used to measure the energy spectrum of fission neutrons produced when a sphere of metallic uranium was irradiated by thermal neutrons.

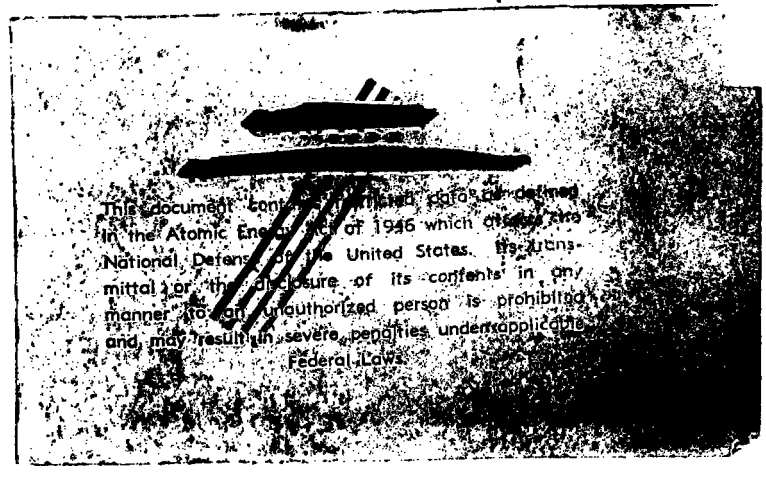

P-271-1

THE ENERGY SPECTRUM OF FISSION NEUTRONS FROM 235

Experimental Arrangement:

A proton beam of 2 MV energy was allowed to fall on a target of metallic lithium, producing neutrons whose energies were of the order of 100 KV. The target was surrounded by paraffin to slow down some of these neutrons, the total quantity of paraffin being about 50 grams. A sphere of metallic uranium, 2 inches in diameter, was placed at one side of the paraffin, and the cloud chamber was placed on the same side at a distance of 6 inches from the uranium. The arrangement is shown in Fig. 1.

The cloud chamber was 26 cm in diameter and of heavy construction to withstand several atmospheres pressure inside. Photographs were taken with a stereoscopic mirror arrangement to allow reprojection of the tracks in space. The illuminated region was 5 cm deep. A strip 9 cm wide extending from front to rear of the chamber was visible in both stereoscopic photographs. Tracks were produced only during the sensitive time of the chamber by adjusting the timing of a shutter in the path of the proton beam.

Data:

In the first run, the cloud chamber was filled with methane to two atmospheres pressure. 1750 photographs were taken with the above arrangement and 600 photographs were taken to see if any neutrons other than fission neutrons were being photographed. The background runs were taken by (a) removing the uranium, (b) by putting lead in place of the uranium, and (c) by reducing the energy of the proton beam below the threshold for production of neutrons in the lithium target. The background was found to amount to only a few percent.

Tracks were measured only when they were within 15° of the direction of the fission neutrons. The angle could not be determined accurately for the shortest tracks so tracks shorter than 1 cm were excluded from the final results. This left the part of the spectrum below 1 MV undetermined. Because of the possibility that a large number of neutrons might be emitted with velocities nearly the same as the velocities of the fission fragments, the energy spectrum between 0.4 and 1.0 MV was investigated in a second run with hydrogen in the cloud chamber to a pressure of 2 atmospheres. 2035 photographs were taken with the uranium in place and 1060 photographs were taken with lead replacing the uranium.

[redacted]

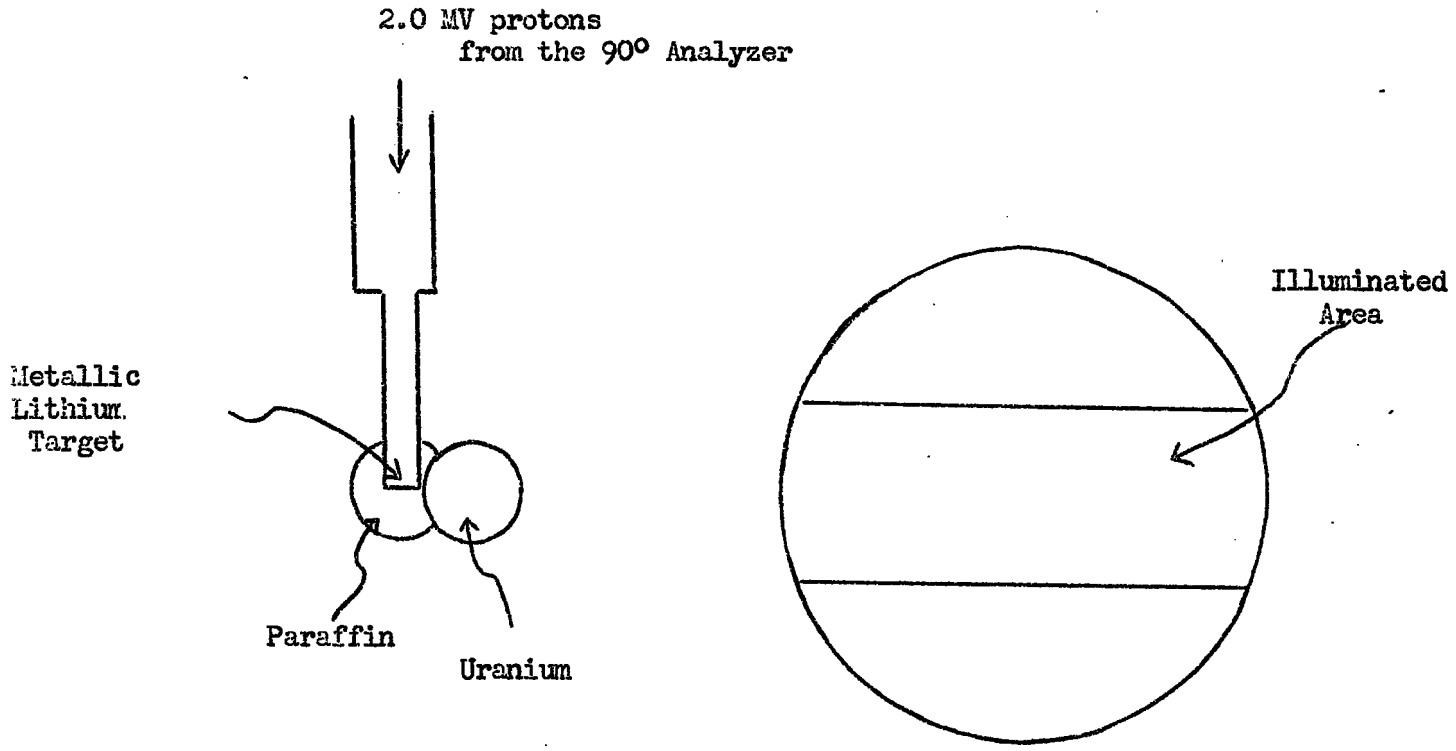

Scale 1:4

FIG. 1

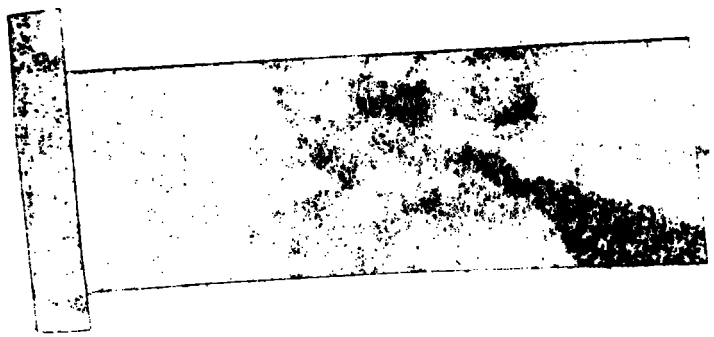

UNCLASSIFIED

UNCLASSIFIED

P-211-3

[redacted]

A third run was taken with the cloud chamber filled with ethane to two atmospheres. About 450 photographs had been taken when the experiment was discontinued. No background runs were included, but the background was small in methane and no serious error is made by assuming that it is the same percentage in ethane.

The lengths of all recoil tracks visible in the photographs were measured to half a millimeter. Tracks which made an angle greater than 15° with the line from the middle of the uranium sphere were excluded. It was also required that both ends of the track be sharp and not too near the walls of the cloud chamber. The lengths in the cloud chamber mixture were converted to lengths in standard air. The stopping power of each cloud chamber mixture of gas and 95% ethyl alcohol vapor was determined from the pressure as read on a Bourdon type gauge when the cloud chamber was expanded and from the atomic stopping powers as given by Livingston and Bethe[1]. At low energies the atomic stopping powers vary rapidly with energy. Therefore, for the hydrogen data, a stopping power curve was plotted and used to change lengths to ranges in standard air. In the other mixtures the stopping power was calculated for 5 cm protons and was considered constant.

The purity of each gas used was checked by a density determination. The density of the methane indicated 13% ethane present. This is about the ratio to be expected if the methane cylinder (supplied by the Ohio Chemical Co.) was actually filled with natural gas.

The Neutron Spectrum

Energy intervals were chosen to be 0.5 MV wide for the methane and the ethane data and 0.2 MV wide for the hydrogen data. The boundary of each interval of the neutron spectrum was reduced by 6.3% to obtain intervals in which the number of recoil protons could be counted. A reduction of 3.5% was required because protons were measured out to 15°, and hence the energies of the protons were on the average less by that amount than the energies of the neutrons which produced them. The further reduction was required because of the apparent unsymmetrical straggling observed when the spectrum of monochromatic neutrons from $C^{12} + D$ was measured in the same cloud chamber[2]. The number of recoil proton tracks in each energy interval was then corrected for (a) the cross-section for n-p collision, (b) geometrical factors, and (c) wall effects in the cloud chamber, to obtain the number of neutrons in the corresponding energy interval.

The cross-section for collision of a neutron with a hydrogen nucleus has been given as a function of energy by Kittel and Breit[3]. Their values were used, the correction factor being normalized to one for a recoil proton of 10 cm range in the cloud chamber mixture.

[redacted]

[redacted]

UNCLASSIFIED

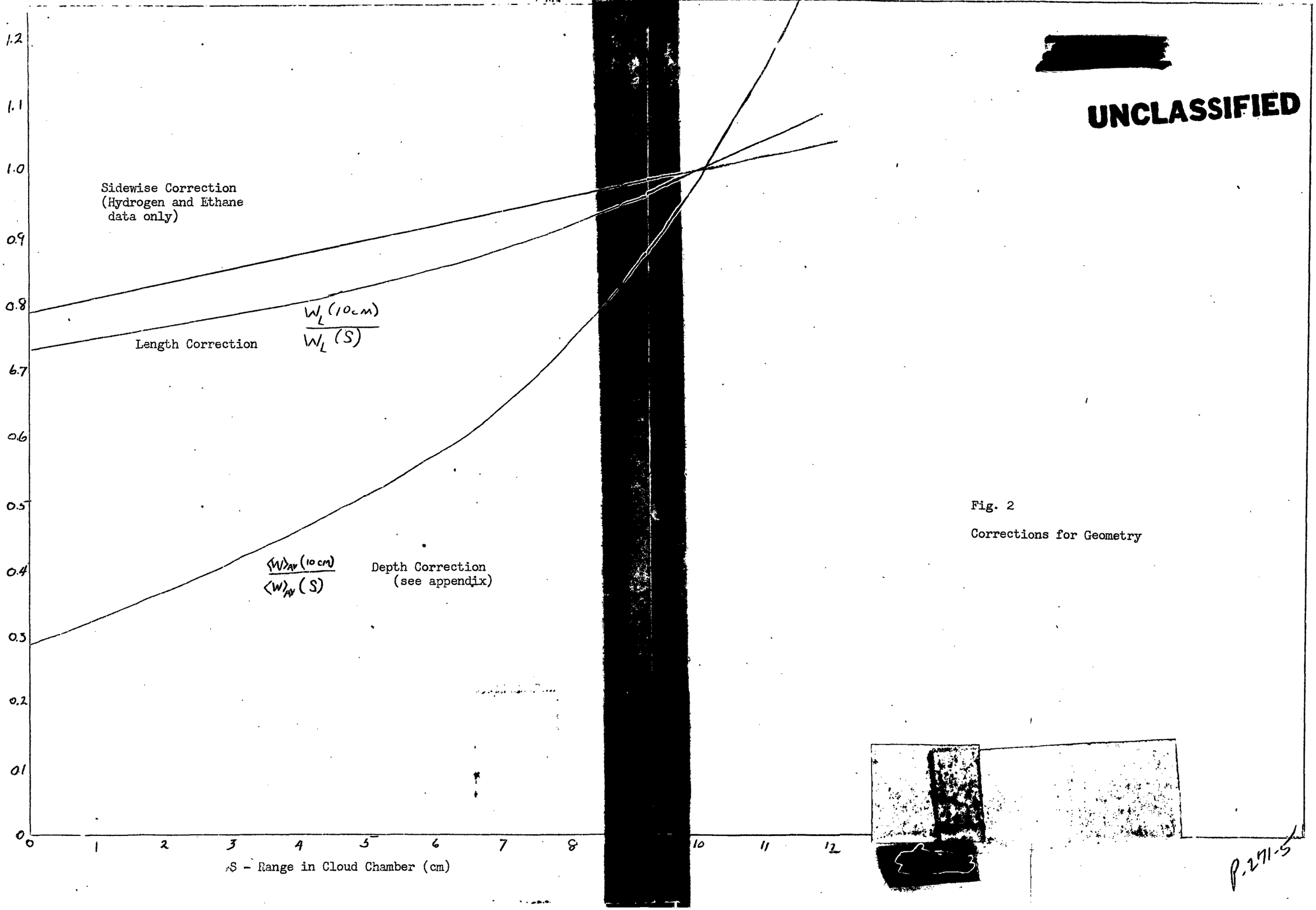

Fig. 2

Corrections for Geometry

P-271-5

Longer recoil protons have smaller probability of being measured because they leave the chamber at the distant wall or at the top and bottom of the illuminated space. If they left the side of the stereoscopic space they could still be measured in one of the photographs. Hence two geometrical corrections were required. The first is for the finite length of the chamber and is given by

$$W_L = (1/L_o) - 1/(L_o + \lambda - S) \qquad (1)$$

where W_L is the probability of observing a track of length S in the rectangular illuminated area of the cloud chamber of diameter λ, (see appendix, Fig. 1). L_o is the distance from the source to the chamber. L_o was 14 cm for all data, and λ was taken as 21 cm because tracks were not measured near the walls.

The correction for the finite depth of the chamber is of the simple form

$$W_d = 1 - (4 S \sin \theta_o) / 3\pi d \qquad (2)$$

if the source is infinitely distant from the chamber. θ_o is the maximum angle that the recoil proton can make with the neutron and still be acceptable for measurement. θ_o was 15° in the present experiment; and d, the depth of the illuminated portion of the chamber, was 5 cm. The above simple expression was the correction factor used for our preliminary reports on the neutron spectrum. However, if the neutron source is not infinitely distant, use of the above expression discriminates against the longer tracks. Evidence that this discrimination was appreciable was the failure of the corrected spectrum taken in the hydrogen run to agree satisfactorily with the corrected methane and ethane data in the region of overlap. Therefore, we undertook to calculate the correction factor which should be used if the neutron source is at finite distance. The derivation of this correction is given as an appendix to this report. The resulting correction factor for our particular experimental arrangement has been evaluated, normalized to one for a 10 cm proton recoil in the chamber, and plotted in Fig. 2. The difference between the new and the old correction factor is quite appreciable.

After the methane data was finished, difficulty was found in measuring tracks which went out of the stereoscopic space on one side so these tracks were excluded in the hydrogen and ethane data. Hence an additional correction was applied to these data. This correction for the finite width of the stereoscopic area is of the same form as the new depth correction (see appendix) except that proper allowance must be made for the fact that tracks leaving one side of the stereoscopic space could still be measured on the other photograph. This correction is also plotted in Fig. 2.

The correction for wall effects was based on our measurements[2] of the monochromatic neutrons from C^{12}/D. In that experiment, performed with

[redacted]

[redacted]

P. 271.6

the same cloud chamber, a flat background was observed on the low energy side of the monochromatic group. The background was believed to be caused by either elastic or inelastic scattering of the neutrons in the walls of the cloud chamber, but its interpretation is not relevant to the present experiment. The number of neutrons in the background was one sixth of the number in the group. (This estimate was made after the data given in reference (2) was recompleted using the new geometry correction which is derived in the appendix of this report.) The assumption was made that this ratio would not change much with the energy of the neutron group. The correction is small for high energies, but it became rather large for the low energies reached in the hydrogen run, and was 20% for the lowest energy interval.

The numbers of recoil protons in each energy interval is tabulated in Tables I, II, and III for methane, hydrogen, and ethane respectively. The corrections are also given and the number of neutrons in each interval.

Table I

Spectrum in Methane

Energy Interval MV	No. Recoil Tracks	No. Back-ground	Corrected for Back-ground	Cross section	Geometry	Wall effects	Relative No. of Neutrons
1.0-1.5	21		21	11.4	3.0	2.4	2.4 ± 0.4
1.5-2.0	18	1	15	9.7	2.9	2.5	2.5 ± 0.7
2.0-2.5	8		8	5.9	2.1	1.8	1.8 ± 0.5
2.5-3.0	8		8	6.6	2.9	2.6	2.6 ± 0.7
3.0-3.5	8		8	7.3	4.2	4.0	4.0 ± 1.0
3.5-4.0	3		3	3.0	2.5	2.4	2.4 ± 1.0
4.0-4.5	3		3	3.3	4.2	4.1	4.1 ± 1.6
>4.5	3		3				
Spectrum in Hydrogen (Table II)							
0.4-0.6	34	3	28	14.8	2.9	1.9	1.9 ± 0.5
0.6-0.8	30	3	24	14.7	3.3	2.4	2.4 ± 0.6
0.8-1.0	21	1	19	13.1	3.5	2.7	2.7 ± 0.6
1.0-1.2	25		25	19.1	6.0	5.4	5.4 ± 0.8
1.2-1.4	11		11	9.1	3.6	3.1	3.1 ± 0.7
1.4-1.6	7		7	6.2	3.2	2.7	2.7 ± 0.8
1.6-1.8	4		4	3.8	2.8	2.3	2.3 ± 0.9
1.8-2.0	2		2	2.0	2.2	1.8	1.8 ± 1.1
>2.0	7		7				

p. 27.7

Table III

Spectrum in Ethane

Energy Interval MV	No. Recoil Tracks	No. Back-ground	Corrected for Back-ground	Cross section	Geometry	Wall Effects	Relative No. of Neutrons
1.0-1.5	22		22	10.1	2.0	1.6	1.6 ± 0.3
1.5-2.0	20	(1)	17	9.3	2.1	1.8	1.8 ± 0.4
2.0-2.5	14		14	8.8	2.2	2.0	2.0 ± 0.4
2.5-3.0	10		10	6.9	2.1	1.9	1.9 ± 0.4
3.0-3.5	8		8	6.2	2.2	2.1	2.1 ± 0.5
3.5-4.0	5		5	4.3	1.9	1.8	1.8 ± 0.6
4.0-4.5	1		1	0.9	0.5	0.5	0.5 ± 0.4
4.5-5.0	1		1	1.0	0.8	0.8	0.8 ± 0.6
5.0-5.5	2		2	2.2	2.7	2.7	2.7 ± 1.3
>5.5	1		1				

A final result for the energy spectrum of fission neutrons was obtained by adding the methane data to the ethane data, the latter being weighted by a factor of two. The two sets of data were based on observation of about equal numbers of tracks, but for a given neutron energy the range of the recoil proton is much less in the ethane and hence uncertainties in the geometrical corrections are less. The number of neutrons between 0.5-1.0 Mv was obtained from the hydrogen data by using the number of neutrons between 1.0 and 2.0 Mv to normalize the value. The final results are given in Table IV and plotted in Fig. 3.

Table IV

Energy Interval (MV)	Relative No. of Neutrons
0.5-1.0	4.6 ±0.9
1.0-1.5	5.6 ±0.7
1.5-2.0	6.1 ±1.3
2.0-2.5	5.8 ±0.9
2.5-3.0	6.4 ±1.1
3.0-3.5	8.2 ±1.5
3.5-4.0	6.0 ±1.5
4.0-4.5	5.1 ±1.8

The error indicated in Tables I-IV is the probable error based on the number of recoil proton tracks observed.

Discussion

The neutron spectrum is to a first approximation flat between 0.5 λ and 4.5 MV. It appears to fall off somewhat at the low energy end, but this point is not emphasized because the amount which it falls off depends upon the wall correction which may have been overestimated to some extent.

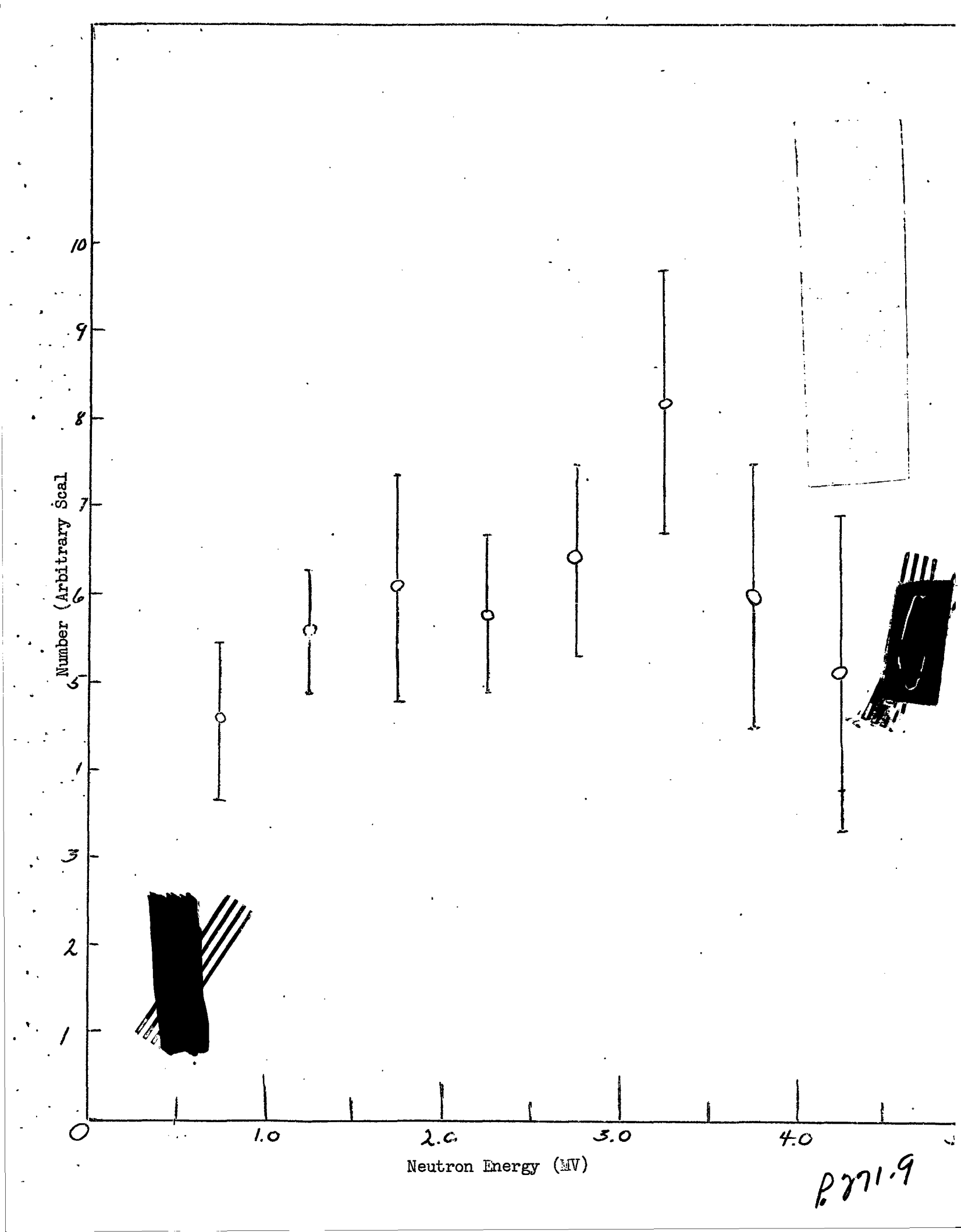
Number (Arbitrary Scal
10
9
8
7
6
5
4
3
2
1
0
1.0
2.0
3.0
4.0
Neutron Energy (MV)

P 271.9

Inelastic scattering in the uranium sphere itself has not been considered in working out the results. If it is as large as has been reported, the true spectrum may slope upward with increasing energy in the energy region here considered.

For our experimental arrangement (Fig. 1), scattering of the fission neutrons in the uranium itself (either elastic or inelastic) would tend to reduce the number of neutrons observed in the cloud chamber. This reduction would exist because the majority of the fission neutrons are produced in the side of the sphere farthest distant from the cloud chamber. The error caused thereby cannot be calculated, but it is unlikely to be serious unless the scattering cross-section of neutrons by uranium is large and varies rapidly with energy.

The presence of the paraffin does not distort the spectrum of neutrons from uranium because it is all "behind" the uranium, and the uranium neutrons would have to be scattered several times in the paraffin to reach the cloud chamber. Also the dimensions of the paraffin are only of the order of the mean free path of fast neutrons. We checked the effect of the paraffin by measuring the increase in ionization in a methane filled electroscope when paraffin was put "behind" the lithium target. Apparently, with the amount of paraffin which we have used, less than several percent of the measured tracks would be of too low energy.

It is certain that the spectrum of fission neutrons extends to energies considerably above 4.5 MV. In each set of data, the number of tracks observed in excess of an upper energy limit have been recorded. These were tracks which started in the gas and were within 15° of the forward direction, but some of them went out of the chamber because of their high energy. Although their numbers were small, they represent a large number of high energy neutrons because the probability of observing such long tracks was very small. In addition, recoil tracks were observed which apparently started in a film of moisture in the front wall and went all the way across the chamber when it was filled with ethane. These tracks require the presence of neutrons of energy greater than 7.6 MV in the fission spectrum.

Because of the high energies involved, the measurement of proton recoil tracks in a cloud chamber cannot give complete results for the spectrum of fission neutrons. A photographic plate might be used to record proton recoil tracks, or a cloud chamber could be used if conditions were such that the tracks of recoiling helium nuclei were measured.

References:

1. Livingston and Bethe, Rev. Mod. Phys 9, 276, (1937)
2. W. E. Bennett and H. T. Richards, CF Report No. 206
3. Kittel and Breit, Phys. Rev. 56, 744 (1939)

p. 771-16

[redacted]

Appendix

A GEOMETRY CORRECTION FOR CLOUD CHAMBER DATA WHEN THE NEUTRON SOURCE IS NOT INFINITELY DISTANT

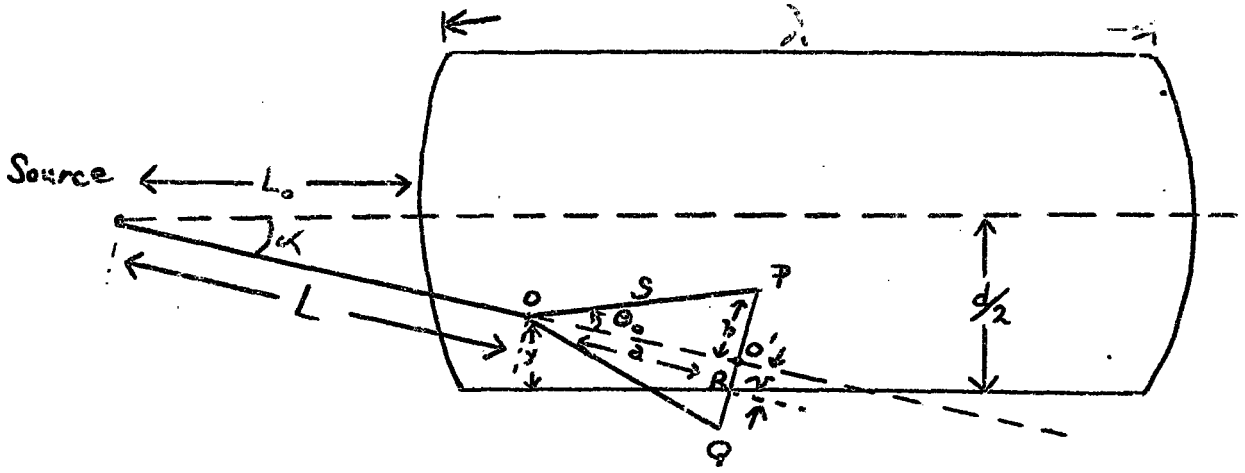

Fig. 1

Notation:

L -- distance from source to scattering center O
L_o -- minimum value of L
y -- distance from edge of illuminated section (bottom or side) to scattering center O
S -- range in cloud chamber of the recoil proton = OP
θ -- angle of recoil proton to incident neutron
θ_o -- maximum acceptable value of θ
a -- S $\cos\theta_o$
b -- S $\sin\theta_o$
d -- depth (or width) of illuminated portion of cloud chamber
λ -- length of illuminated portion of cloud chamber
α -- angle which the neutron makes with respect to a line from the source which bisects the chamber.
ν -- O'R

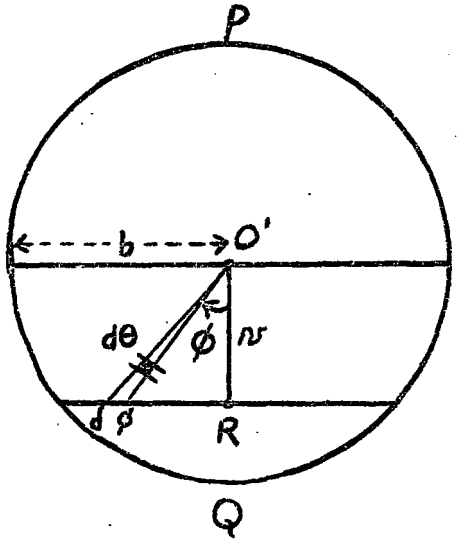

Fig. 2 - End view of PO'Q of Fig. 1

[redacted]

[redacted]

p. 371.11

Let $k\sigma$ be the number of recoil protons scattered from 0 into the solid angle subtended by circle PQ, and let $k\sigma'$ be the number of recoil protons scattered from 0 into the solid angle subtended by circle segment PO'R. Then the probability that a recoil proton, scattered from 0 into the solid angle subtended by circle PQ, will end within the illuminated portion of the chamber (and hence be acceptable for measurement) is

$$W = k\sigma' / k\sigma = \sigma'/\sigma \tag{1}$$

But

$$k\, d\sigma = \cos\theta \sin\theta\, d\theta\, d\phi \tag{2}$$

Hence

$$k\sigma = \int_0^{2\pi}\int_0^{\theta_0} \cos\theta \sin\theta\, d\theta\, d\phi = \pi \sin^2\theta_0 \tag{3}$$

From Fig. 1 and Fig. 2 (appendix),

$$k\sigma' = \frac{k\sigma}{2} + 2\left(\int_0^{\phi_I}\int_0^{\theta_0} + \int_0^{\phi_{II}}\int_0^{\theta_{II}}\right) \cos\theta \sin\theta\, d\theta\, d\phi \tag{4}$$

$$= \frac{k\sigma}{2} + \sin^2\theta_0 \sin^{-1}\left(\frac{v}{b}\right) + \frac{v}{\sqrt{a^2+v^2}} \tan^{-1}\left(\frac{b^2-v^2}{a^2+v^2}\right)^{\frac{1}{2}} \tag{5}$$

Since

$$\text{Sin}\ \phi_I = \frac{v}{b}$$

$$\sin\theta_{II} = \left(1+\frac{a^2}{v^2}\cos^2\phi\right)^{-\frac{1}{2}}$$

$$\tan\phi_{II} = \left(\frac{b^2 - v^2}{v^2}\right)^{\frac{1}{2}}$$

Therefore:

$$W = \frac{k\sigma'}{k\sigma} = \frac{1}{2} + \frac{1}{\pi} \sin^{-1}\left(\frac{v}{b}\right) + \frac{1}{\pi \sin^2\theta_0} \frac{v}{\sqrt{a^2+v^2}} \tan^{-1}\left(\frac{b^2-v^2}{a^2+v^2}\right)^{\frac{1}{2}} \tag{6}$$

The above expression is valid for $|v| \leq b$; and because of the relationship between v and y (see below), it holds for $0 \leq y \leq y'$. From Fig. 1 (appendix)

$$v = \frac{d}{2} \sec\alpha - (L+a)\tan\alpha \tag{7}$$

and

$$\sin\alpha = (d/2 - y)/L \tag{8}$$

For the usual experimental geometry, it is a good approximation to set $\cos\alpha = 1$ in expression (7). The resulting expression combined with (8) gives

$$v = By - A \tag{9}$$

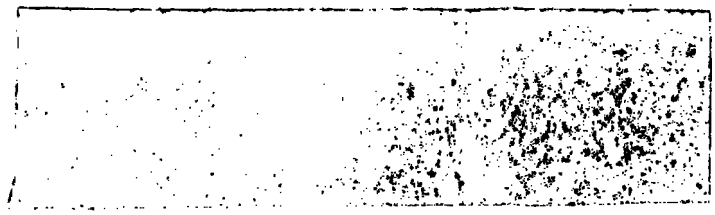

p. 7114

where

$$A = da/2L \tag{10}$$

$$B = (L + a)/L \tag{11}$$

Therefore, when v = b,

$$y\ (= y') = (b + A)/B \tag{12}$$

The expression for the average value of W for scattering centers between y = 0 and y = d/2,

$$\langle W \rangle_{av} = (2/d)\left[y'\bar{W} + (d/2 - y')x\ 1 \right] , \tag{13}$$

requires that we first know the mean value of W in the interval $0 \leq y \leq y'$. This mean value of W is denoted by $\bar{W}$ in expression (13).

For the calculation of $\bar{W}$ we have

$$\bar{W} = (1/y')\int_0^{y'} W\, dy = 1/(b + |v'|)\int_{-v'}^{b} W\, dv \tag{14}$$

and since by (9), (-v') = A when y = 0, the result is .

$$\bar{W} = 1/(b + A)\int_A^b W\, dv \tag{15}$$

All terms of the last integral, (15), are easily evaluated except the one involving

$$\int f(v)\ \tan^{-1}\left[(b^2 - v^2)/(a^2 + v^2)\right]^{\frac{1}{2}} \tag{16}$$

However, the maximum value of the arctangent function in (16) occurs when v = 0. For the present experiment this maximum value is the tangent of 15°. For angles less than 15° there will be less than a 2% difference between the angle and its tangent. Hence to integrate (16), we replace the arctangent function by the tangent itself. Expression (15) then results in

$$\bar{W} = \tfrac{1}{2} + \frac{1}{\pi(b+A)}\left[\frac{b\pi}{2} - A \sin^{-1}\left(\frac{A}{b}\right) - \sqrt{b^2 - A^2}\ (1 + \csc^2\theta_o) + \frac{S}{2\sin^2\theta_o} \log\frac{S + \sqrt{b^2 - A^2}}{S - \sqrt{b^2 - A^2}} \right] \tag{17}$$

Substituting (17) and (12) in (13) gives

$$\langle W \rangle_{av} = 1 - \frac{A}{dB} - \frac{2A}{\pi dB} \sin^{-1}\left(\frac{A}{b}\right) - \frac{2\sqrt{b^2 - A^2}}{\pi dB}(1 + \csc^2\theta) + \frac{S}{\pi dB\ \sin^2\theta} \log \frac{S + \sqrt{b^2 - A^2}}{S - \sqrt{b^2 - A^2}} \tag{18}$$

Since A and B are each functions of L, expression (18) is not yet applicable to the observed distribution of recoil protons. Because it is difficult to average (18) with respect to L, the following procedure was adopted. First, average values of L (weighted according to the inverse

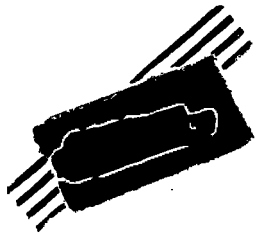

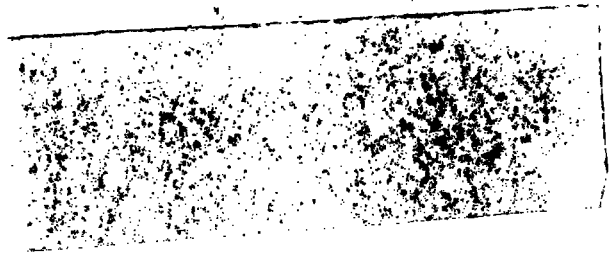

square law) for five different track lengths, S, were computed:

$$\bar{L} = 1/(\lambda - S) \int_{L_o}^{L_o+\lambda-S} (k/L^2)\, L\, dL = (k/\lambda - S) \log\left(\frac{L_o+\lambda-S}{L_o}\right) \qquad (19)$$

The constant k is determined by the condition that $\bar{L} = L_o$ when $S = \lambda$. The result is

$$\bar{L} = \left[\frac{L_o(L_o+\lambda-S)}{\lambda-S}\right] \log\left(\frac{L_o+\lambda-S}{L_o}\right) \qquad (20)$$

The mean values of L thus calculated were then used in (18) to compute $\langle W \rangle_{av}$ for five different track lengths S. The resulting correction factors normalized to one for a 10 cm track are plotted on Fig. 2 of the main portion of this report.